

## Monte Carlo simulation calculation of the critical coupling constant for two-dimensional continuum $\phi^4$ theory

Will Loinaz\*

*Institute for Particle Physics and Astrophysics, Physics Department, Virginia Tech, Blacksburg, Virginia 24061-0435*

R. S. Willey†

*Department of Physics and Astronomy, University of Pittsburgh, Pittsburgh, Pennsylvania 15260*

(Received 4 December 1997; revised manuscript received 10 June 1998; published 10 September 1998)

We perform a Monte Carlo simulation calculation of the critical coupling constant for the continuum two-dimensional  $(\lambda/4)\phi^4$  theory. The critical coupling constant we obtain is  $[\lambda/\mu^2]_{crit} = 10.26_{-0.04}^{+0.08}$ .  
[S0556-2821(98)07219-1]

PACS number(s): 11.10.Kk, 05.50.+q, 11.15.Ha

### I. INTRODUCTION

The two-dimensional  $\phi^4(\phi^4)$  field theory, specified by the (Euclidean) Lagrangian

$$\mathcal{L}_E = \frac{1}{2}(\nabla\phi)^2 + \frac{1}{2}\mu_0^2\phi^2 + \frac{\lambda}{4}\phi^4, \quad (1)$$

has solutions in a symmetric phase in which the discrete symmetry of the Lagrangian,  $\phi \rightarrow -\phi$ , is manifest, i.e.,  $\langle\phi\rangle=0$  and there is no trilinear coupling. It also has solutions in a broken symmetry phase with  $\langle\phi\rangle \neq 0$  and induced trilinear couplings proportional to  $\langle\phi\rangle$ .

There exist both elegant heuristic [1] and rigorous [2] mathematical proofs of the existence of this phase structure, but there is no rigorous result for the critical value of some coupling constant which separates these two phases. There do exist numerous approximate calculations, and in the case of the lattice model (lattice spacing  $a > 0$ ), the critical line in the  $\mu_0^2, \lambda$  plane which separates the two phases is known to some numerical accuracy by Monte Carlo simulation.

For the Euclidean quantum field theory (EQFT), which is the continuum limit ( $a \rightarrow 0$ ) of the lattice model, the first step is to specify what finite dimensionless coupling constant is to be used to parametrize the solutions and for which we are to determine the critical value.

For the lattice model, these considerations are straightforward. There are two parameters,  $\mu_0^2, \lambda$  in  $\mathcal{L}_E$ , and there is the lattice spacing  $a$ . In  $d=2$  both  $\mu_0^2$  and  $\lambda$  have dimension mass squared. (We assume the infinite volume limit,  $L \rightarrow \infty$ .) So there are two independent dimensionless parameters which may be taken to be the two Lagrangian parameters measured in units of inverse lattice spacing squared,

$$\lambda_{\ell} = \lambda a^2, \quad \mu_0^2_{\ell} = \mu_0^2 a^2. \quad (2)$$

In this parametrization, the phase diagram of the lattice model consists of the critical line in the  $\mu_0^2_{\ell}, \lambda_{\ell}$  plane, determined by Monte Carlo simulation (Fig. 1).

The situation for the EQFT is more complicated. There is an infinite mass renormalization. The bare mass parameter has to be tuned to infinity as the continuum limit is taken,  $\mu_0^2 \sim \mu^2 \ln(1/a)$ , where  $\mu^2$  is some finite renormalized mass squared. Thus  $\mu_0^2$  cannot be used as a parameter of the continuum solution. In  $d=2$ , the field strength and coupling constant renormalizations ( $Z_{\phi}, Z_{\lambda}$ ) are finite and can be disregarded in the study of the phase structure of the theory. Furthermore, since the dimensionful coupling constant  $\lambda$  is independent of  $a$ , and  $\mu_0^2$  diverges only logarithmically with  $a$ , both  $\lambda_{\ell}, \mu_0^2_{\ell}$  go to zero in the continuum limit,  $a \rightarrow 0$ . That is, the EQFT limit is the single point at the origin of the  $\mu_0^2_{\ell}, \lambda_{\ell}$  plane in Fig. 1. Taking the limit  $a \rightarrow 0$  reduces the number of independent dimensionless parameters from two to one.

The required mass renormalization can be written as a simple reparametrization of  $\mathcal{L}_E$  (1). Let

$$\mu_0^2 = \mu^2 - \delta\mu^2. \quad (3)$$

Then

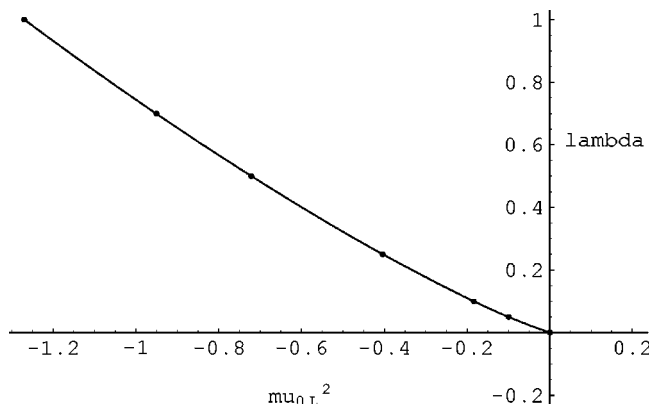


FIG. 1. Phase transition line in the  $\lambda_{\ell}, \mu_0^2_{\ell}$  plane.

\*Email address: loiniz@vt.edu

†Email address: willey@vms.cis.pitt.edu

$$\mathcal{L}_E = \frac{1}{2}(\nabla\phi)^2 + \frac{1}{2}\mu^2\phi^2 + \frac{\lambda}{4}\phi^4 - \frac{1}{2}\delta\mu^2\phi^2. \quad (4)$$

There is still a substantial freedom of choice in the definition of the finite renormalized mass parameter,  $\mu^2$ . The ultraviolet,  $\ln(1/a)$ , dependence of  $\mu_0^2$  is moved entirely to the counterterm  $\delta\mu^2$ , but the separation of the finite part of  $\mu_0^2$  into  $\mu^2$  and  $\delta\mu^2$  is only determined when a renormalization condition is specified. The dimensionless effective coupling constant  $f_{\mu^2} = \lambda/\mu^2$  then manifestly depends on the choice of renormalization condition which fixes the finite part of  $\delta\mu^2$ . For example, we could take  $\mu^2 = m_*^2$ , the pole mass, by choice of renormalization condition

$$0 = G^{-1}(p^2 = -m_*^2) \quad (5)$$

and dimensionless coupling

$$g = \frac{\lambda}{m_*^2}. \quad (6)$$

A closely related choice, convenient for lattice Monte Carlo measurement, is to take  $\mu^2 = m'^2$ , defined by the renormalization condition

$$m'^2 = G^{-1}(p^2 = 0) \quad (7)$$

and

$$g' = \frac{\lambda}{m'^2}. \quad (8)$$

In fact, neither of these choices provide a dimensionless coupling constant whose value distinguishes between the two phases of the theory—because the renormalization conditions themselves do not distinguish between the two phases. Either renormalization condition, Eqs. (5) or (7), can be implemented perturbatively in either the symmetric phase or the broken symmetry phase. The phase has to be specified by ansatz,  $\langle\phi\rangle = 0$  or  $\langle\phi\rangle \neq 0$ , so that one can perturb about the correct stable vacuum. Then  $g$  or  $g'$  can take on arbitrarily small values in either phase.

A dimensionless coupling constant whose critical value separates the two phases is provided by choosing the mass renormalization to be equivalent to normal ordering the interaction in the interaction picture in the symmetric phase. From Eqs. (1) and (3),

$$G^{-1}(p^2) = p^2 + \mu_0^2 + \Sigma_0(p^2) = p^2 + \mu^2 + \Sigma(p^2) \quad (9)$$

and, for  $\mu^2 > 0$ ,

$$\Sigma(p^2) = 3\lambda A_{\mu^2} - \delta\mu^2 + \text{two-loop}. \quad (10)$$

$A_{\mu^2}$  in the continuum limit is the ultraviolet divergent Feynman integral:

$$A_{\mu^2} = \int \frac{d^2p}{(2\pi)^2} \frac{1}{p^2 + \mu^2}. \quad (11)$$

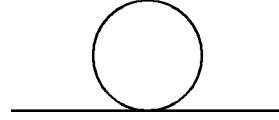


FIG. 2. Leaf diagram.

On the lattice,

$$A_{\mu^2} = \frac{1}{N^2} \sum_{k_1=1}^N \sum_{k_2=1}^N \frac{1}{\mu^2 + 4\sin^2 \pi k_1/N + 4\sin^2 \pi k_2/N}. \quad (12)$$

The ‘‘leaf’’ diagram (Fig. 2) which gives the integral  $A_{\mu^2}$  is the only divergent Feynman diagram of the theory in  $d=2$ .

Thus the renormalization condition

$$\delta\mu^2 = 3\lambda A_{\mu^2} \quad (13)$$

removes all ultraviolet divergence from the perturbation series based on the renormalized parametrization given by Eqs. (4) and (13).

$$\begin{aligned} \mathcal{L}_E &= \frac{1}{2}(\nabla\phi)^2 + \frac{1}{2}\mu^2\phi^2 + \frac{\lambda}{4}\phi^4 - \frac{3}{2}\lambda A_{\mu^2}\phi^2 \\ &= \frac{1}{2}(\nabla\phi)^2 + \frac{1}{2}\mu^2\phi^2 + \frac{\lambda}{4}\phi^4;_{\mu^2}. \end{aligned} \quad (14)$$

In the last normal ordered form, we have dropped a constant piece. The dimensionless coupling constant suggested by Eq. (14) we denote simply by  $f$ :

$$f = \frac{\lambda}{\mu^2}. \quad (15)$$

Since the normal order prescription in Eq. (14) is relative to the vacuum of the symmetric phase theory, we may investigate the possibility of a critical value of the coupling constant  $f$ . Using Eq. (15), the first line of Eq. (14) may be rewritten as

$$\mathcal{L}_E = \frac{1}{2}(\nabla\phi)^2 + \frac{1}{2}\mu^2(1 - 3fA_{\mu^2})\phi^2 + \frac{f\mu^2}{4}\phi^4. \quad (16)$$

On the lattice (fixed  $a > 0$ ),  $A_{\mu^2}$  is finite, and we can argue that for small enough  $f$ , the exact effective potential is well approximated by the classical effective potential with its single minimum at  $\phi_{cl} = 0$ . For large  $f$ , the coefficient of  $\phi^2$  in Eq. (16) becomes negative, suggesting a transition to the broken symmetry phase. However the argument falls short at this point because for strong coupling one cannot argue that the effective potential is well approximated by its tree level form. The argument was completed by Chang [1] by constructing a duality transformation from the strong coupling regime of Eq. (14) to a weakly coupled theory normal ordered with respect to the vacuum of the broken symmetry phase.

TABLE I. Analytic approximations of the critical value of  $f$ .

Approximation	Result	Reference
Non-Gaussian variational	6.88	[6]
Discretized light-front	7.316, 5.500	[8], [9]
Coupled cluster expansion	$3.80 < f_c < 8.60$	[7]
Connected Green function	9.784	[5]
Gaussian effective potential	10.211	[1]
	10.272	[5]

There are several attempts in the literature (see Table I) to compute the critical value,  $f_c$ , by various analytic approximations, with a rather large spread of answers. In this paper we report an accurate numerical value by Monte Carlo simulation. The first step is to obtain the critical line in the  $\mu_{0\prime}^2, \lambda_{\prime}$  plane. This determines  $\mu_{0\prime}^2(\lambda_{\prime})_{crit}$  (see Fig. 1). Recall that these values are infinite volume extrapolations of finite volume Monte Carlo data. Then, combining Eqs. (3) and (13), we obtain

$$\mu_{0\prime}^2 = \mu_{\prime}^2 - 3 \lambda_{\prime} A_{\mu^2}. \quad (17)$$

In the infinite volume limit  $A_{\mu^2}$  (12) has the integral representation

$$A_{\mu^2} = \int_0^{\infty} dt \exp(-\mu_{\prime}^2 t) (\exp(-2t) I_0(2t))^2. \quad (18)$$

For any point away from the origin, Eqs. (17), (18) can be solved numerically to determine  $\mu_{\prime}^2(\lambda_{\prime})_{crit}$ . This is then extrapolated into the origin to determine

$$f_c = \lim_{\lambda_{\prime}, \mu_{\prime}^2 \rightarrow 0} \left. \frac{\lambda_{\prime}}{\mu_{\prime}^2} \right|_{crit}. \quad (19)$$

## II. SIMULATIONS

The Monte Carlo simulation is based on the lattice action which regularizes the continuum theory (1):

$$\mathcal{A} = \sum_{\vec{n}} \left\{ \frac{1}{2} \sum_{\nu=1}^d (\varphi(\vec{n} + \vec{e}_{\nu}) - \varphi(\vec{n}))^2 + \frac{1}{2} \mu_{0\prime}^2 \varphi(\vec{n})^2 + \frac{\lambda_{\prime}}{4} \varphi(\vec{n})^4 \right\}. \quad (20)$$

Periodic boundary conditions were imposed on  $N \times N$  square lattices with  $N = 32, 64, 128, 256$ , and 512. To reduce critical slowing down, our updating algorithm consisted of a standard Metropolis update (i.e., with a symmetric transition matrix) alternating with a cluster algorithm updating the embedded Ising model. The procedure is similar to that of Brower and Tamayo [3], but we substitute a Wolff-type single-cluster algorithm [10] for the Swendsen-Wang multiple-cluster algorithm used there.

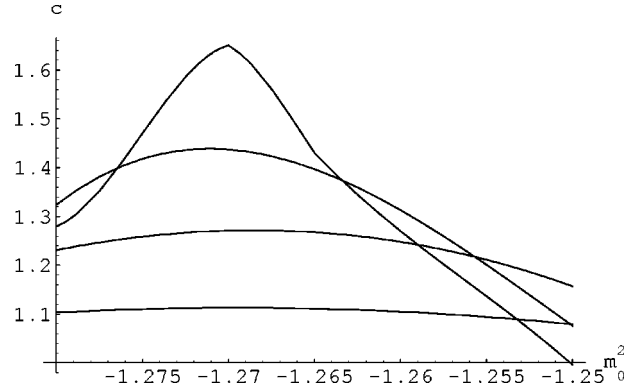


FIG. 3. Plots of  $C_H$  vs  $\mu_{0\prime}^2$ . From lowest to highest, curves are for  $L = 32, 64, 128, 256$ .

Measurement of lattice quantities was performed every ten Metropolis+cluster cycles. Each data collection run consisted of  $10^4$  to  $10^5$  measurements, after an initial thermalization of at least  $10^4$  cycles. To assess the effective number of statistically independent measurements, the integrated autocorrelation time ( $\tau_{INT}$ ) was calculated for each run,

$$\tau_{INT} = \frac{1}{2} + \sum_{i=1}^M \frac{s(i)}{s(0)} \quad (21)$$

where  $s(i)$  is the autocorrelation separated by  $i$  measurements and  $M$  is some number of measurement such that  $s(M)$  is essentially noise. The largest  $\tau_{INT}$  measured in our simulations was 8 measurements (80 update cycles) and was typically much smaller. Thus, in every case the thermalization time exceeded  $100\tau_{INT}$ , so we expect that our lattices were well thermalized before we began collecting data. We also tried to measure the exponential autocorrelation time  $\tau_{EXP}$  from the first few (time) autocorrelation functions, but these did not appear to fall off as a single exponential. As expected, however, the measured values were slightly smaller than the corresponding  $\tau_{INT}$  for that run. As a result of the small  $\tau_{INT}$  and large number of measurements, statistical errors are typically quite small, generally smaller than the systematic errors in the determination of the critical line in the  $\lambda_L, \mu_L^2$  plane for finite volumes and in the extrapolation to the infinite-volume limit.

For each size lattice, we looked at  $\lambda_{\prime} = 1.0, 0.7, 0.5, 0.25, 0.1$  and 0.05, and for each  $\lambda_{\prime}$  scanned in  $\mu_{0\prime}^2$ , starting in the symmetric phase and ending in the broken symmetry phase. We used two diagnostics to determine the critical value of  $\mu_{0\prime}^2$ . The first is that value of  $\mu_{0\prime}^2$  which produced the maximum of the variance of the action (specific heat), which should diverge as  $C_H \sim \ln|\mu_{0\prime}^2 - \mu_{0\prime,c}^2|$  as lattice size  $L \rightarrow \infty$  [4]. This is illustrated in Fig. 3, where we give the plots of  $C_H$  vs  $\mu_{0\prime}^2$ , for  $\lambda_{\prime} = 1.0$ , for lattice sizes  $L = 32, 64, 128, 256$ . The narrowing and strengthening of the peak as  $L$  increases is seen. One can also see that estimate of critical  $\mu_{0\prime}^2$  in the infinite volume is very close to  $-1.27$  for  $\lambda_{\prime} = 1.0$ .

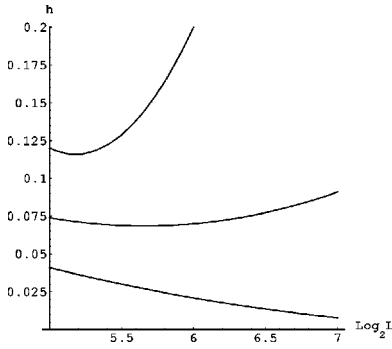


FIG. 4. Plot of  $h$  vs  $\log_2(L)$ ; from top to bottom curves are for  $\mu_{0\ell}^2 = -1.26, -1.27, -1.28$ .

The second is based on the shape of the histogram of the distribution of  $\langle \varphi \rangle$ . In the symmetric phase with  $L \gg \xi$ , the spatial correlation length, the probability distribution of  $\langle \varphi \rangle$  should be a single peak centered about zero, while in the broken-symmetry phase with  $L \gg \xi$ , the distribution should consist of two identical peaks at equal distance from  $\langle \varphi \rangle = 0$ . For a fixed value of  $\mu_{0\ell}^2$ , histograms of  $\langle \varphi \rangle$  will approach one of these distributions for  $L$  sufficiently large. To quantify the bimodality of the distribution, we bin the data and define  $h$  to be the ratio of the number in the central bin to the largest number in any outlying bin. For a histogram which is a single peak centered about zero,  $h > 1$ . For a histogram which is two peaked, around  $+\langle |\varphi| \rangle$  and  $-\langle |\varphi| \rangle$ ,  $h \ll 1$ . The diagnostic for a given  $\mu_{0\ell}^2$  is the behavior of  $h$  as the lattice size is increased. For  $\mu_{0\ell}^2$ 's which lead to symmetric phase in the infinite volume limit,  $h$  increases with  $L$  until it exceeds one. For  $\mu_{0\ell}^2$ 's which lead to broken symmetry phase in the infinite volume limit,  $h$  is rapidly decreasing with increasing  $L$ . For a narrow range of  $\mu_{0\ell}^2$  around the infinite volume critical value, this behavior may not stand out until one gets to quite large lattices. This is illustrated in Fig. 4 which shows interpolating curves for  $h(L)$ , for  $\lambda_\ell = 1.0$ , for  $\mu_{0\ell}^2$  fixed at  $-1.26, -1.27, -1.28$ . From the behavior of these curves, it is clear that for  $\mu_{0\ell}^2 = -1.26$ , the infinite volume limit will be in the symmetric phase ( $h > 1$ ); while for  $\mu_{0\ell}^2 = -1.28$ , the infinite volume limit will be in the broken symmetry phase ( $h \rightarrow 0$ ). The curve for  $\mu_{0\ell}^2 = -1.27$  is much closer to critical behavior than are the curves for  $\mu_{0\ell}^2 = -1.26$  or  $-1.28$ . Figures 3 and 4 are the basis for the first entry in Table II,  $\mu_{0\ell}^2 (\lambda_\ell = 1.0)_{crit} = -1.270(3)$ . The other entries are obtained by similar analysis.

### III. ANALYSIS

In the second column of Table II we give our estimates of the critical value of  $\mu_{0\ell}^2$  for each of the values of  $\lambda_\ell$  listed above, extrapolated to the infinite volume limit. (They are the input for Fig. 1.) They may be compared with the values found by Toral and Chakrabarti [4] seven years ago, extrapo-

TABLE II. Determination of the phase transition line for different  $\lambda_\ell$ .

$\lambda$	$\mu_{0c}^2$	$\mu_c^2$	$\frac{\lambda}{\mu^2}$
1.0	-1.270(3)	0.0980(8)	10.204(80)
0.7	-0.9516(8)	0.06844(23)	10.228(33)
0.5	-0.7210(10)	0.0489(3)	10.225(63)
0.25	-0.4035(5)	0.0242(2)	10.33(8)
0.10	-0.1838(5)	0.009615(140)	10.40(15)
0.05	-0.0998(3)	0.00492(9)	10.16(19)

lating from much smaller lattices. Within the estimated errors they are consistent, except for the smallest  $\lambda_\ell$ , which is closest to the continuum limit and requires larger lattices to accommodate both large  $L$  and small  $a$ . In the third column of Table II, we give the corresponding critical values of  $\mu^2$  as determined from Eqs. (17) and (18), and in the fourth column we give the corresponding values of  $\lambda/\mu^2$  which are to be extrapolated to the infinite volume continuum limit.

In order to get a feel for the systematic errors, we have done the extrapolation in a number of different ways. We have plotted  $\mu^2$  vs  $\lambda$  and taken the inverse of the slope at the origin to determine the critical value of  $f$ . This is shown in Fig. 5. Note that the data fall very well on a straight line ( $\chi^2 = 0.65$ ) which passes through the origin within the estimated error. As a small variation on this, we have redone the fit forcing the line to go exactly through the origin. The two values of  $f_c$  determined in this manner are 10.23(3) and 10.24(3), respectively. Alternatively, we have extrapolated the values of  $\lambda/\mu_c^2$  to the continuum limit ( $\lambda_\ell = \lambda a^2 \rightarrow 0$ ) as shown in Fig. 6.

$$\frac{\lambda}{\mu_c^2(\lambda)} = f_c + \text{const} \times \lambda a^2. \quad (22)$$

The fit to a linear function of  $\lambda_\ell$  accommodates the discretization error of order  $a^2$ .

This extrapolation gives  $f_c = 10.32(7)$ .

Although the errors originated as statistical errors in simulations on finite lattices the subsequent extrapolations have introduced systematic errors larger than the statistical errors. Thus the assignment of the final result and errors are just

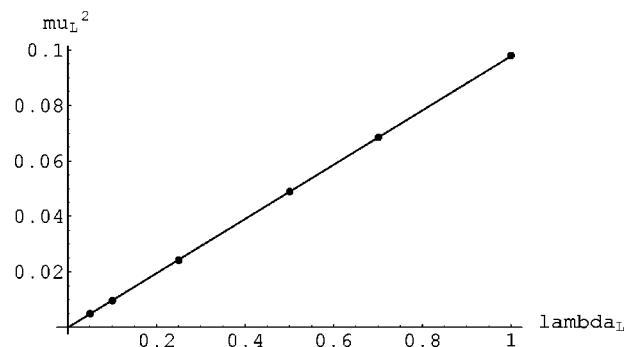


FIG. 5. Plot of phase transition line in the  $\mu_l^2, \lambda_l$  plane.

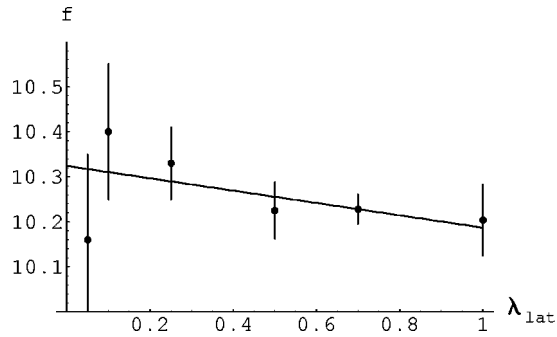


FIG. 6. Extrapolation to determine the critical value of  $f$ .

based on the consistency of the above numbers. We conclude that the critical value of  $\lambda/\mu^2$  is  $10.26^{+.08}_{-.04}$ .

#### IV. ANALYTIC APPROXIMATIONS

The above result may be compared with various approximate analytic calculations. The simplest approach would be to consider the one-loop effective potential. In  $d=2$  this is

$$V_{\text{eff}} = \frac{\mu^2}{2} \phi^2 + \frac{\lambda}{4} \phi^4 - \frac{\mu^2 + 3\lambda \phi^2}{8\pi} \times \left( \ln \frac{\mu^2 + 3\lambda \phi^2}{\kappa^2} - 1 \right). \quad (23)$$

With the assignment  $\kappa^2 = \mu^2$ , this  $V_{\text{eff}}$  gives a first-order phase transition for  $f_c = 6.6$ .

A compendium of nonperturbative analytic approximate calculations has been compiled in Ref. [5]. We include these results for purposes of comparison with the numerical MC simulation result.

There is also the issue of the order of the phase transition. According to the Simon-Griffiths theorem [11], the phase transition is second order. In the analytic approximations, the order of the phase transition is determined; the one-loop effective potential and the Gaussian effective potential predict a first-order phase transition, while the other correctly predict a second-order phase transition. In our numerical calculation of the critical coupling constant, we have made no effort to distinguish between weakly first-order and second-order phase transitions.

#### V. CONCLUSIONS

We have calculated an accurate numerical value of the critical coupling constant using Monte Carlo simulation. With this we can evaluate the accuracy of analytic approximation methods. It is interesting to observe that the Gaussian effective potential result for the critical coupling is consistent with the accurate numerical result, although it gives incorrectly the order of the phase transition.

#### ACKNOWLEDGMENTS

We would like to thank Professor R. Mawhinney for writing some of the programs used in this project. W. Loinaz was supported in part by the U.S. Department of Energy under the Grant No. DE-FG05-92ER40709-A005. R. Willey thanks Professor Carlos Aragao de Carvalho for hospitality at CBPF Brazil where this work was begun.

- 
- [1] Shau-Jin Chang, Phys. Rev. D **13**, 2778 (1976); Shau-Jin Chang, Phys. Rev. D **16**, 1979(E) (1977).
  - [2] J. Glimm and A. Jaffe, *Quantum Physics: A Functional Integral Point of View* (Springer-Verlag, New York, 1981).
  - [3] R. C. Brower and P. Tamayo, Phys. Rev. Lett. **62**, 1087 (1989).
  - [4] Raul Toral and Amitabha Chakrabarti, Phys. Rev. B **42**, 2445 (1990).
  - [5] J. M. Häuser, W. Cassing, A. Peter, and M. H. Thoma, Z. Phys. A **353**, 301 (1996).
  - [6] L. Polley and U. Ritschel, Phys. Lett. B **221**, 44 (1989).
  - [7] M. Funke, U. Kaulfuss, and H. Kümmel, Phys. Rev. D **35**, 621 (1987).
  - [8] A. Harindranath and J. P. Vary, Phys. Rev. D **36**, 1141 (1987).
  - [9] A. Harindranath and J. P. Vary, Phys. Rev. D **37**, 1076 (1988).
  - [10] U. Wolff, Phys. Rev. Lett. **62**, 361 (1989).
  - [11] B. Simon and R. G. Griffiths, Commun. Math. Phys. **33**, 145 (1973).